SEMARAK ILMU PUBLISHING

Journal of Advanced Research in Applied Mechanics

Journal homepage:
https://semarakilmu.com.my/journals/index.php/appl_mech/index
ISSN: 2289-7895

Advancing Rehabilitation Accuracy: A Robotic-Human-Like Controller for Continuous Passive Motion with Natural Behavioural Responses

Aufa Chehlah[1], Paramin Neranon[1,*], Pornchai Phukpattaranont[2], Nattha Jindapetch[2]

[1] Department of Mechanical and Mechatronics Engineering, Faculty of Engineering, Prince of Songkla University, Hat Yai, Songkhla, 90110, Thailand
[2] Department of Electrical and Biomedical Engineering, Faculty of Engineering, Prince of Songkla University, Hat Yai, Songkhla, 90110, Thailand

ARTICLE INFO

Article history:
Received 26 June 2024
Received in revised form 4 August 2024
Accepted 12 August 2024
Available online 30 August 2024

Keywords:
Continuous Passive Motion (CPM); Surface Electromyography (sEMG); Dynamic force estimation; Ridge-Polynomial Model; Artificial Neuron Network (ANN); Support Vector Machine (SVM)

ABSTRACT

Conventionally, researchers have primarily focused on developing gravity-compensation robots without considering the voluntary resistant force in continuous passive motion (CPM) therapy. This leads to critical limitations in robot-assisted therapy compared to conventional therapy administered by therapists, particularly in terms of generating natural behavioural responses in patients. To address this limitation, our proposed technique aims to investigate model-based dynamic force estimation specifically related to intrinsic muscular force in order to develop a robotic-human-like controller for CPM therapy. We conducted an estimation of the muscular force based on surface electromyography (sEMG) signals using Ridge Polynomial, Artificial Neural Network (ANN), and Support Vector Machine (SVM) approaches. Strategic preprocessing and model optimization procedures were implemented. The optimized results demonstrate that ANN exhibits slightly superior performance enhancing the accuracy and precision with its quicker testing time. Moreover, the substantive results demonstrate a notable comparison between the use of conventional gravity compensation and our novel technique which integrates both intrinsic muscular force and gravity compensation. It reveals that our approach yields calculated voluntary forces that more closely approximate to the actual values in comparison to the conventional method. In conclusion, this research makes a significant contribution to the development of a smart robotic controller offering high-accuracy measurement of voluntary forces for CPM therapy, thereby facilitating natural behavioural responses.

1. Introduction

Currently, Stroke is a significant contributor to severe disability among adults all over the world [1]. This condition arises from reduced blood that flows to the brain, which prevents brain tissue from obtaining oxygen and nutrients. Consequently, the affected regions of the brain may experience cellular death, leading to decreased functionality. The stroke symptom may affect movement disorders in patients. To enhance a patient's quality of life for such individuals, exercise-based

* *Corresponding author.*
E-mail address: paramin.n@psu.ac.th

https://doi.org/10.37934/aram.124.1.8198

therapy is necessary to facilitate the rewiring of neurological pathways associated with motor function. Subsequently, the muscle functionalities are able to be gradually better restored. This procedure strictly is under supervision by medical professionals and therapists [2,3].

Moreover, the global trend towards an aging population may consequently increase the demand for therapists to aid patients. Therefore, in response to this impending burden in the future, ongoing research studies have introduced various advanced physical rehabilitation-assisted devices. Robotic devices employed for the rehabilitation of upper limbs can be typically classified into many groups for specific movements such as systems assisting shoulder, elbow, forearm, wrist, finger, or whole arm movements etc. [2–5]. Among these devices, Continuous Passive Motion (CPM) devices, which are relatively simple exoskeleton robots, are particularly used to facilitate significant recovery of forearm and elbow movements in patients [6,7]. Numerous scientific studies provide evidence of the effectiveness of CPM training and it demonstrates significant improvements in muscle strength and overall recovery [1,4,7].

Throughout the treatment course, therapists typically perform to gradually increase the range of motion by approximately 5-7 degrees per day in both active and passive flexion and extension [1–4]. During the treatment process, therapists have the capability to apply naturally suitable force in accordance with the resistant force generated by patients in the presence of high intensity of pain. It can be said that during the treatment process when patients experience intense pain, they may instinctively apply ‘voluntary force’ to resist the rehabilitation movement, aiming to protect themselves from potential physical harm. In response, it is crucial for the therapist to promptly react by adjusting the lower range or lower speed of motion.

Contrastingly, a variety of robotic researchers [8–13] have primarily focused on developing gravity-compensation robots without considering the voluntary resistant force exerted by patients in CPM therapy. Therefore, compared to conventional therapy administered by therapists, robot-assisted therapy consequently shows critical limitations in generating natural behavioural responses in patients [8].

Our research team was initially driven by the challenge to develop naturally behavioural responses in assistive robots during the treatment. Therefore, a series of experiments using a one-degree-of-freedom CPM robot shown in Figure 1 was carried out. To measure the force applied by the subject perpendicular to the test rig, a multi-axis force sensor was attached to the robot's arm link. Through our experimental procedures, which involved instructing subjects to apply resistant force against the movement and not to apply force, we have significantly observed that the test rig is affected by various factors, including the ‘voluntary resistant force’ exerted by the patient, the ‘gravitational force’ acting on the forearm [9–15], and the opposing ‘intrinsic muscular force’ of the forearm. The intrinsic muscular force is the dynamic force generated by the internal muscles themselves during muscle fibre contraction, irrespective of voluntary effort.

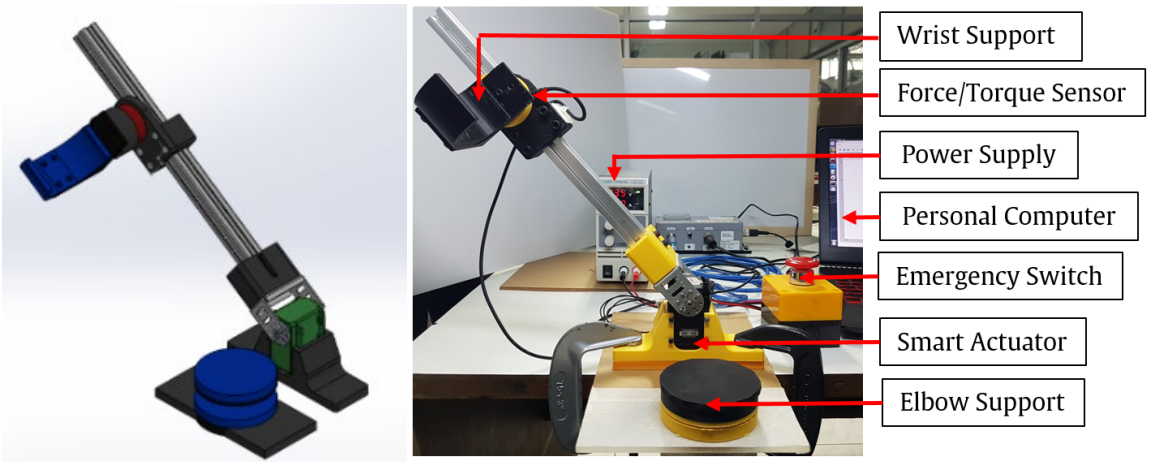

Fig. 1. The design CPM assisting robot

After an extensive review [8–15], it has been determined that there is a notable research gap concerning the topic of intrinsic muscular force in CPM therapy. Model-based dynamic force estimation regarding intrinsic muscular force during exercise-based therapy is scarce. The primary objective of this research is to emphasize the necessity for further examination to expand our understanding of intrinsic muscular force. By doing so, we aim to enhance the accuracy and precision in measuring the voluntary effort exerted by patients during the CPM tests.

The subsequent sections of the research present the details of the proposed study. To begin, the design of a robot and controller is capable of executing force-position control. Subsequently, the force estimation model is carefully developed, following a step-by-step process to create the machine learning model. This is accompanied by a thorough comparison of algorithms in the pre-processing stage, followed by training and testing to retune the model until optimal performance is achieved. Lastly, the integration of the proposed model with the robot control system is executed, culminating in comprehensive performance testing to validate its functionality and effectiveness.

2. The CPM Robotic System Identification

An upper-limb CPM rehabilitation machine is a device that helps a therapist actively manipulate the elbow and forearm in a rotational manner, aiming to restore joint movement [1–5]. The repetitive movements can significantly enhance the stroke patient's muscle functionality or reduce bleeding and increase synovial fluid around the joint for postoperative patients [16–19]. In addition, robotic devices are capable of performing passive and continuous training exercises to rehabilitate joint limitations or joint stiffness who have undergone joint surgery or stroke patients [8,9]. Gao, *et al.,* [20] stated that the outcomes of the CMP therapy demonstrated stroke patients' joint muscles stronger. Driscoll *et al.,* [14] also recommended that it is important to immediately apply passive continuous motion after injury or operation to avoid the cause of the patient's undue pain. Technically, passive therapy requires no patient effort. In the clinical session, an effective training period is around 30-40 minutes and the maximum range of motion is around 125° with the moving velocity between 0.5-5°/s as suggested by Kaewboon *et al.,* [21].

A designed CPM robot has been strategically researched based on a conceptual guideline for a robotic human-like controller for natural, behaviour-based, CPM rehabilitation. This motivates the design of gravity and dynamic intrinsic muscular force compensation to produce the required tracking accuracy of the voluntary resistant effort in real-time interaction. That means if a patient's fatigability, discomfort or pain of skeletal muscles occurs during the therapy process, the intelligent

CPM robot's movement will be reasonably responsive according to the voluntary resistant force applied to the motorized machine against the training movement.

However, this is a crucial challenge in the development of seamless human-robot interaction (HRI), since the robotic control system is further complicated by the dynamic force nature of the muscle contraction and active patient intention response [16–19]. Thus, this study necessitates a very careful design of the behavioural control strategy in order to conduct an effective HRI and strictly protect the human subject from the risk of harm or injury by the CPM robot.

2.1 Design of a Rotational CPM Robotic System

In order to be able to significantly modify its real-time path according to the patient's voluntary effort, an appropriate human-like control strategy for the CPM robot has to be therefore developed. This requires first understanding how the therapist naturally reacts to a patient serving a unique purpose in helping the human from the risk of injury by the robot. The initial study and observation in healthcare were carried out. This process was strictly supervised by the doctors of physical therapy and expert therapists in the rehabilitation centre. Our research team had to strictly follow the guidelines of the WMA Declaration of Helsinki-ethical principles for medical research involving human subjects [22].

After clearly understanding the detail of the rehabilitation context from the Southern Medical Rehabilitation Centre at the Songklanakarin Hospital, Songkhla, Thailand, a conceptual guideline for robotic behaviour-based control can be strategically designed. Additionally, understanding the musculoskeletal system leads to benefits for the development of the robot control architecture of the CPM device.

The designed CPM device can be illustrated in Figure 1. A single rotational DOF offers circular-path-based therapy movement. The test rig provides a mechanical link with an armed supporter to support and rotates the patient's forearm with a pivot point at the elbow joint. The main links were fabricated using aluminium profile and ABS plastic materials since this makes a more lightweight robotic platform and ensures durability and robustness. As the difference of physical lengths of the human arms, firstly the pivot point and length of the rotating link can be effortlessly adjustable for individual suitable positions of a patient.

A smart servo actuator, namely Dynamixel MX-106, can control its velocity precisely as a speed tracking system with a high-resolution contact-less encoder of 4096 pulses per revolution (PPR). The maximum power of the motor is approximately 90 Watts with a torque of 10 Nm. Proportional Integral Derivative (PID) control [23] can be directly used into its servo's built-in microcontroller. This allows a programmer to control the speed and strength of the motor's response using the Robot Operating System (ROS) along with a sampling rate of 50Hz through serial communication.

The human-applied force acting on the robot's rotating mechanism is initially collected in real-time by an ATI Mini40 force/torque sensor. The sensor is associated with an ATI net box and communicates to the PC running ROS via TCP/IP communication with an update rate of 100Hz. The measuring spans of the ATI force and torque are ±80N with 0.02N resolution and ±4Nm with 0.0005Nm resolution, respectively. To improve accuracy of force measurement, the force sensor has to be initially calibrated using a transducer stiffness matrix according to the default sensor reference frame.

Surface electromyography (sEMG) signals reflect the electrical activity of skeletal muscles and contain information about the structure and function of muscles which particularly make different parts of the body move [5,24]. Therefore, sEMG can be used to predict human muscle force in HRI with strong probability. A MYO armband with 8-channel electrode sensors was chosen to detect the

sEMG signals around the human arm in real-time. The sampling rate of the electrodes is approximately 200 Hz which is suitable to measure the human sEMG signals [25]. This was confirmed by Liang *et al.,* [26] in which the frequency of the sEMG signals captured from the human arm is generally around 20–500 Hz. Moreover, a safety system is a crucial issue in haptic HRI. This facilitates an effective human-machine interaction (HMI) as it involved control software and a stand-alone emergency stop button, which can immediately activate once a fail-safe mode occurs.

The overall control block diagram of the robot-assisted rehabilitation system will be expressed in Section C. The next section describes the kinetic and kinematic characteristics of the HMI while performing elbow joint CPM rehabilitation.

2.2 Impedance Characteristic of The Human Arm in CPM

The human arm impedance can be investigated based on the study of Raman *et al.,* [27,28] using dynamic modelling analysis. The human arm is mechanically presented as a spring-dashpot-and-mass system. The HMI system can be schematically depicted in Figure 2. Frictionless assumptions are often made to simplify complex mechanical systems, making mathematical analysis and modelling more controllable. It allows for easier calculations and theoretical predictions. In this study, the friction levels are significantly lower compared to the torque generated by the motor; consequently, it can be assumed that the frictionless pin joint was undertaken.

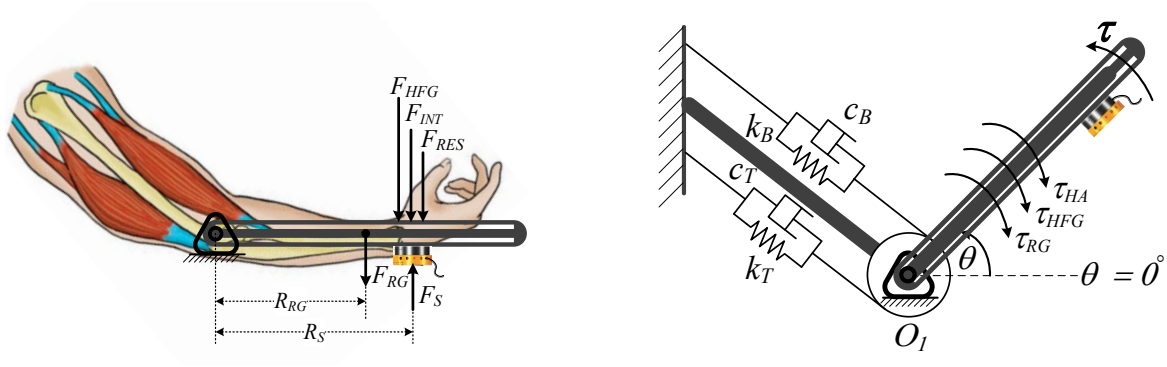

(a) (b)

Fig. 2. Schematic of human arm impedance on the HMI system (a) Free body diagram of the force interaction with the robot (b) Free body diagram of the human arm with the robot

According to the key abbreviations used in Figure 2, their terminology and definitions of the relevant parameters can be expressed as the patient's voluntary resistant force (F_{RES}) which is defined as a force directly applied against the circular movement of CPM (when the patient feels any restriction or pain during the therapy). The corresponding torque is represented by τ_{RES}. Forearm intrinsic muscular force (F_{INT}) is defined as the dynamic force naturally generated by internal muscles themselves during muscle fibre contraction. The corresponding torque is τ_{INT}. Measured force (F_S) is defined as the tangential force directly measured by the multi-axis ATI force sensor based on its coordinate frame.

Forearm gravitational force (F_{HFG}) is defined as the force of the gravity of the human forearm and its direction is toward the ground. Its corresponding torque is τ_{HFG}. Similarly, the gravitational force of the robot link attached by the force sensor (F_{RG}) is also defined as the force of the gravity of the CPM rotating link. The corresponding torque can be written as τ_{RG}, respectively. The net arm torque (τ_{HA}) is generally developed by shortened or lengthened muscles, which can be calculated by

summing τ_{RES} and τ_{INT} together. Finally, the external torque produced by the smart Dynamixel motor can be presented as τ, which can smoothly actuate and rotate the human arm.

By considering all force acting to the force sensor attached to the tip of the link, thus the measured force F_S as shown in Figure 2(a) can be derived as: $F_S = (F_{HFG} + F_{INT} + F_{RES})$. This voluntary resistant force which will is undertaken in the robotic position-based force control to offer the compliant-behavioural-based motion in the HRI task can be estimated as the following equation.

$$F_{RES} = F_S - [F_{HFG} + F_{INT}] \tag{1}$$

where, F_{HFG} can be computed by $F_{HFG}(n) = m_{HFG}gcos\theta(n)$. The human forearm can be represented as $m_{HFG}$and the gravitational acceleration is approximately 9.83 m/s^2, and θ is the rotational angle of the human forearm, respectively.

According to the interaction between the human subject and the motorized CPM rehabilitation machine as depicted in Figure 2(b), using the direct equivalent to Newton's second law based on rotational kinematic analysis offers the following equation.

$$\tau(n) - \tau_{HA}(n) - \tau_{HFG}(n) - \tau_{RG}(n) = I\ddot{\theta}, \tag{2}$$

where the arm's angular position and its corresponding velocity and acceleration are represented by θ, $\dot{\theta}$ and $\ddot{\theta}$, respectively.

The elbow torque τ_{HA} is regulated regarding the contraction of muscles related to muscle flexion and extension while interacting with a HRI task. Subsequently, an overall simple second-order equation in the time domain was used as the model for the arm dynamics and arm moment can be mathematically expressed by the following equations.

$$\tau_{HA}(t) = [c_B(t) + c_T(t)]\dot{\theta}(t) + [k_B(t) + k_T(t)]\theta(t) \tag{3}$$

The arm impedance consists of c_B, c_T, k_B and k_T representing damping factors and stiffness parameters of biceps brachii, and triceps brachii, respectively. Substituting Eq. (3) to Eq. (2) gives:

$$\tau(n) - [c_H(n)]\dot{\theta}(t) - [k_H(n)]\theta(n) - \tau_{HFG}(n) - \tau_{RG}(n) = I\ddot{\theta} \tag{4}$$

The next step is to transform the continuous-time domain (t) into a discrete-time domain at every sampling time with the individual discrete number samples represented by n. It is initially assumed.

$\dot{\theta}(n) = \frac{\theta(n)-\theta(n-1)}{T}$ and $\ddot{\theta}(n) = \frac{\dot{\theta}(n)-\dot{\theta}(n-1)}{T}$ provide:

$$\tau(n) = a_1\theta(n) + a_2\theta(n-1) + a_3\theta(n-2) + \tau_{HFG}(n) + \tau_{RG}(n) \tag{5}$$

where, $a_1 = (\frac{I+c_H(n)T+k_H(n)T^2}{T^2})$, $a_2 = (\frac{2I+c_H(n)T}{T^2})$ and $a_3 = (\frac{I}{T^2})$, respectively.

According to the equations derived above, one of the most challenges is to estimate unknown impedances in the human dynamic model while performing flexion or extension. Then, to address this challenge, it becomes necessary to strategically estimate model-based dynamic force specifically related to intrinsic muscular and gravitational forces.

2.3 Real-Time Force Control for the Robotic CPM System

A conceptual control block diagram of the robot-assisted elbow rehabilitation system can be demonstrated in Figure 3. This was designed based on the studies by Neranon and his colleagues [16–19]. The ROS system is running on a host computer and serves as robotic control-based data processing, in which position-based force control [18,19,29] was adopted to deal with the unconstrained moving path of the assistant robot. This type of control is composed of two important control loops, which refer to the inner PID position control and outer PI force control systems as suggested by Neranon [16,29]. In the meantime, the control algorithm is directly modified by a pre-defined trajectory, simultaneously to update a new point of the robot's moving path.

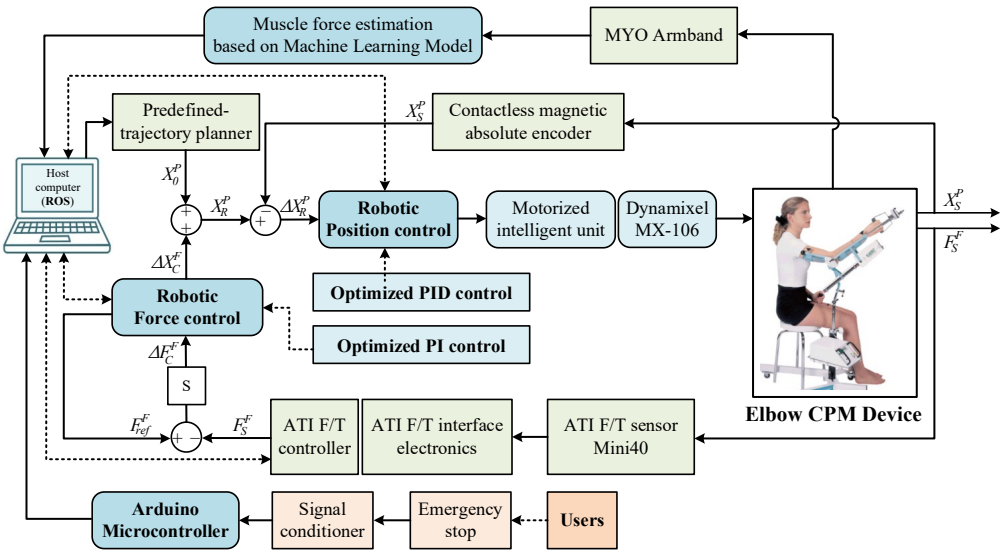

Fig. 3. Control block diagram of the CPM robot system

The robotic control system for elbow rehabilitation, as shown in Figure 3, was initially inspired by the work conducted by Neranon and collaborators [16-19]. To ensure smooth human-robot interaction, the system adopts position-based force control. This control strategy consists of two loops: an inner loop for PID position control and an outer loop utilizing PI control for managing forces during operation. It operates via the ROS system on a host computer, handling both robotic control and data processing aspects. ROS provides an array of packages and tools facilitating seamless communication between sensors and actuators.

Additionally, it offers a visual interface, enhancing the system's real-time monitoring capabilities. The system employs a Dynamixel MX-106 smart servo actuator known for its precise velocity control. This actuator interfaces with ROS, allowing PID control implementation. Operating at a 20Hz sampling rate, it delivers a maximum power of around 90 Watts and offers a stall torque of 10 Nm. Real-time collection of human-applied force is facilitated by an ATI Mini40 force/torque sensor, communicating with ROS via TCP/IP at 1000Hz. To estimate muscle force using sEMG signals, data is gathered at a fitting 200 Hz sampling rate through an MYO armband containing 8-channel sEMG sensors. Ensuring safety, the system includes emergency stop buttons. These buttons allow external devices to trigger context-based safety stops swiftly in emergency situations.

The next section will describe how to apply machine learning in a historical-data-based algorithm computation that can provide more accuracy of predicted outcomes. The estimation of model-based dynamic force in HMI can be accomplished by using Machine Learning (ML) [30,31], whereas in this context, sEMG [32] serves as a promising approach for predicting these internal forces. Due to the

complexity of the sEMG investigation in human muscles, the Ridge regression model [33,34], Artificial Neuron Network (ANN) [24,35,36] and Support Vector Machine (SVM) approaches [24,37] were utilized in this study. These will be fully detailed in Section III. These supervised learning algorithms are capable of facilitating the robotic system which can completely compensate for gravity and dynamic intrinsic muscular forces to produce the required tracking accuracy of the voluntary resistant effort in real-time HRI.

3. Development of Machine Learning Model Approaches Used in Human Muscle Force Estimation

As extensively reviewed, there are several research studies on sEMG-based force estimation approaches using different algorithm models such as Ridge regression model, ANN and SVM approaches. Technically, there are three main steps [38] in the machine learning process used for sEMG-based force estimation, namely data collection, data preprocessing, and regression model and hyperparameters tuning method [39]. Details of each step are as follows.

3.1 Data Collection System

There are three different types of relevant data used in this study i.e. 1) eight channels of sEMG signals captured from the human arm muscles, 2) acting force applied by a patient, and 3) angular positions of the CPM test rig. The sEMG and force signals were synchronously detected at 200 Hz, whereas the rotational angle parameter was measured at the lower rate of 20 Hz. The experimental apparatus was set up, as depicted in Figure 4, and the research study was strictly conducted according to the guidelines of the Declaration of Helsinki [22].

A total of twenty healthy participants, consisting of 10 males and 10 females, were involved in the CPM forearm therapy test. It ensured that the test results were statistically significant as suggested by a set of pilot studies. All subjects had to become familiar with the test rig with 5 repetition sets to avoid the effects of human learning. To identify relevant internal forces, each participant was then instructed to perform all assigned tasks without any voluntary effort at all times. Pulling, pushing, twisting or bending the handle was not allowed. Initially, the human subjects were seated in comfortable positions and placed the forearm and elbow as the arm supporter as depicted in Figure 4(a). Figure 4(b) depicts the positions of the electrode channels.

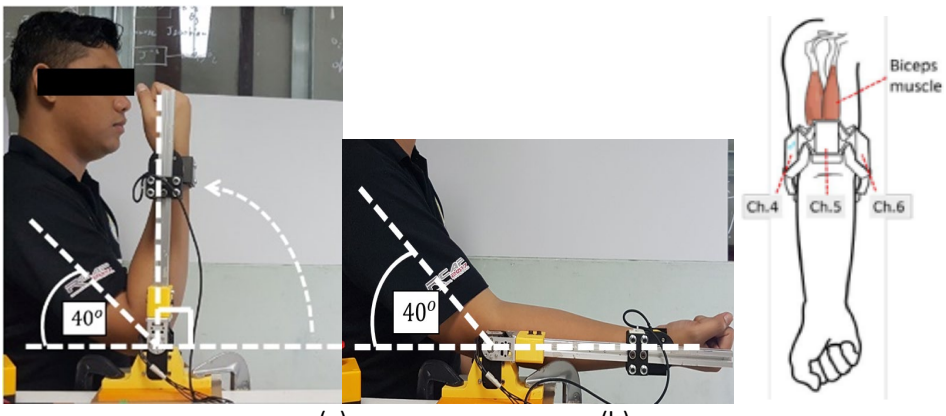

(a) (b)

Fig. 4. (a) The experimental setup for the robot-assisted CPM rehabilitation (b) the electrode positions of the eight channels of sEMG signals

In Figure 4(b), the electrode channels used were channels 3-6, which were placed on the biceps brachii muscles, and channels 1, 2, 7, and 8, which measured sEMG signals from the triceps brachii muscles. Once the timer trigger was activated, the CPM robot moved the human forearm at a constant angular velocity of 3 rpm. It started from the initial position of 0 degrees and moved towards the target position of 90 degrees. During the test cycle, we monitored and recorded a set of approximately 100,000 raw data samples in real-time. These samples were then divided into two main groups for the machine learning process. The first group, called the in-sample group, consisted of 80% of the data and was used for algorithm training and development. The second group, called the out-sample group, comprised 20% of the data and was used to evaluate the performance of the estimated algorithms.

3.2 Preprocessing Process

After gathering the relevant data, it becomes necessary to employ data mining techniques to transform all acquired information into desirable formats. In accordance with the feature extraction procedure [38], [40], the commonly used and highly regarded methods for estimating force based on sEMG signals [21], [32] are recommended, namely root mean square (RMS) and mean absolute value (MAV) [41]. To identify the selected features that significantly impact the performance of the model fitting, it is crucial to apply the statistical chi-square method. This method allows for the examination of significant differences among the relevant parameters obtained from a random sample.

3.2.1 First preliminary: feature scoring analysis

Consequently, the first preliminary has been carried out to identify whether each input feature is chiefly correlated to the target feature, namely applied force, or not. The feature scoring technique was employed to evaluate the comparisons among 8 RMS features, 8 MAV features derived from the sEMG signals, and an angular position feature in relation to the force feature. The technique utilizes statistical measures to assess the correlation between input and output parameters, making it valuable for force prediction. The results of the feature scoring technique, which are presented in Table 1, demonstrate the calculated scores.

The test results in Table 1 clearly indicate two distinct categories. The first group consists of selected features with high-rating scales, exceeding 2,300. These selected features include position features, the RMS and MAV features derived from channels 3, 4, 5, and 6 of the sEMG signals. On the other hand, the second group represents an unselected set of features from channels 1, 2, 7, and 8, with significantly lower rating scores. Notably, the significant electrodes are positioned directly on the biceps brachii muscles in an array configuration. To further reduce data variance, the next step involves implementing feature scaling techniques such as normalization and standardization. This ensures that the magnitudes of the selected features are scaled to the same range, resulting in improved performance of the fitting model.

Table 1
The comparative results of feature scoring with the chi-square method

Descriptions	Features	Scores
Selected Features	Position	621505.52
	RMS 5	8778.80
	MAV 5	7826.42
	RMS 6	6194.17
	MAV 6	5246.69
	RMS 4	4939.93
	MAV 4	4008.60
	RMS 3	3211.43
	MAV 3	2395.62
Unselected Features	RMS 7	604.98
	MAV 7	560.56
	RMS 2	166.80
	RMS 1	128.36
	MAV 2	128.00
	MAV 1	80.13
	RMS 8	40.29
	MAV 8	27.62

3.3 Model Selection and Hyperparameter Tuning

The development of machine learning algorithms involves constructing appropriate mathematical models to accurately predict the target variables. This process encloses three key procedures: training, validation, and testing. In this research, the regression model initially used was the Ridge polynomial model. The Ridge model is a method addressing multi-collinearity, which occurs when there are high intercorrelations among input variables in a multiple regression model. By employing this model, the researcher can effectively determine the optimal utilization of each input parameter for accurate predictions. The algorithm, derived from the linear Ridge model, is capable of predicting non-linear data. It offers advantages such as coefficient shrinkage, reduced model complexity, and decreased training and testing time. The pipelined technique was utilized to integrate the algorithm with the polynomial feature generation method, ensuring the assessment of dataset quality and distribution.

3.3.1 Second preliminary: comparative performance analysis of model fitting tools using Ridge polynomial model

The test involved utilizing the Ridge polynomial model to compare the performance of different model fitting tools. The normalization process was performed to reduce the range of the data to a fixed range, typically between 0 and 1 (or -1 to 1). It is particularly effective when the data distribution is non-Gaussian or when the standard deviation is small. This is normally useful when features have different scales and units. The normalization process follows a specific equation.

$$x_i^{`} = \frac{x_i - min(x)}{max(x) - min(x)}. \quad (6)$$

Standardization or Z-score normalization involves rescaling the dataset's feature to have the properties of a Gaussian distribution, where μ and σ are the mean and its corresponding standard

deviation, respectively. Standardization transforms data to have a mean of 0 and a standard deviation of 1. It can be calculated as follows:

$$z = \frac{x-\mu}{\sigma} \tag{7}$$

Hence, the tests were carried out and categorized into 3 groups as follows: (1) non-scaling feature or without normalising data, (2) normalization-based feature scaling, and (3) standardization-based feature scaling. The tests were repeatedly undertaken under several window sizes of 50, 100 and 150 samples, respectively.

A series of statistical forecasting tests were conducted under various preprocessing scenarios, and the results are presented in Table 2. The performance of the machine learning model in fitting the dataset was assessed based on the RMSE, with a lower magnitude indicating better performance. The results indicate that employing standardization-based feature scaling in conjunction with the Ridge polynomial model consistently yielded lower RMSE values, approximately 0.33 N, across all window sizes. Therefore, this preprocessing approach will be utilized in the subsequent experiments.

The Ridge regression model was initially employed and tuned by adjusting the feature weights. However, after an extensive review of muscle force estimation using sEMG signals, it became evident that Artificial Neural Networks (ANN) and Support Vector Machines (SVM) have been widely recommended by numerous researchers [2,24,37].

Table 2
The comparison of the preprocessing results using the Ridge-Polynomial model

Window size	Case 1: Non-scaling Feature Selected Feature				Case 2: Standardization Selected Feature				Case 3: Normalization Selected Feature			
	Train		Test		Train		Test		Train		Test	
	RMSE	SD	RMSE	SD	RMSE	SD	RMSE	SD	RMSE	SD	RMSE	SD
50	0.568	0.019	0.683	0.070	0.341	0.011	0.380	0.034	0.452	0.023	0.525	0.063
100	0.535	0.019	0.673	0.045	0.337	0.013	0.386	0.030	0.439	0.020	0.559	0.044
150	0.511	0.022	0.671	0.055	0.334	0.011	0.393	0.019	0.437	0.019	0.571	0.045

The model selection process involves choosing a suitable machine learning model that captures the relationship between the input and output training dataset. However, one challenge is effectively using different models with hyperparameters. For example, in SVM, exploring different kernels such as linear, nonlinear, polynomial, Gaussian, and Radial Basis Function (RBF) is crucial. The model parameter configuration greatly influences the predictive performance of the data.

Optimizing or tuning hyperparameters in machine learning tasks plays a vital role in controlling the learning process to achieve an optimized model. Common techniques for hyperparameter optimization include grid search, random search, and Bayesian optimization [42]. However, grid search has limitations in terms of computational resources and processing time, while random search may not always yield the best optimization for each model. To overcome these limitations, this research successfully implemented a Bayesian optimizer using the scikit-optimizer, as recommended by previous researchers [9–11].

3.3.2 Third preliminary: optimization of SVM and ANN models using Bayesian optimizer

The third-preliminary tests were conducted to optimize SVM and ANN models using a Bayesian optimizer. The SVM models utilized various kernel functions including linear, nonlinear, polynomial, RBF, and sigmoid. The same set of sEMG signals and muscle force variables were repeatedly trained

to compare the forecasting performance of SVM models under different kernel conditions. By employing the optimizer to identify the global optimization point, it was determined that the RBF kernel function yielded the best performance, which aligns with the findings of Tanausavapol *et al.,* [24]. This optimized RBF kernel will be further used in the subsequent tests in Session 4.

Optimizing the ANN model involves several steps, including (1) determining the optimal number of hidden layers, (2) selecting an appropriate activation function, and (3) choosing a suitable solver for weight optimization. The performance of the model is evaluated by comparing its predictive capabilities. This comparison is typically based on RMSE values, with lower variation indicating better performance in predicting force.The number of hidden layers in the ANN model was adjusted within the range of one to four layers, based on suggestions from various researchers [3,12,13]. Four different activation functions were tested, including (1) the identity function (no operation), (2) the logistic sigmoid function, (3) the hyperbolic tangent function, and (4) the rectified linear unit function. The main solvers used in the tests were quasi-Newton methods, stochastic gradient descent, and a stochastic gradient-based optimizer, which is typically employed in large datasets [14].

The results of optimizing the ANN model using the Bayesian optimizer are shown in Table 3. The RMSE values indicate the accuracy of estimating muscle force based on sEMG signals. The results demonstrate that the RMSE values are consistently close, ranging from approximately 0.329 to 0.338 N for data training and from 0.365 to 0.368 N for data testing. This confirms that all models accurately estimate muscle forces based on sEMG signals. Upon analysing the model tuning time, it was observed that the single-hidden layer configuration outperformed the multi-hidden layer configurations. The tuning process for this configuration took only 22 minutes. Consequently, the 'Adam' solver and 'logistic' activation functions were selected for the ANN model. During model testing, the optimized ANN model achieved an RMSE of 0.366 N, with a standard deviation of 0.031 N. These optimized ANN and SVM models were then used in the subsequent experiments outlined in the following session.

Table 3
The results of comparing ANN parameters using hyperparameter tuning

ANN parameters	1 Hidden layer size	2 Hidden layer size	3 Hidden layer size
Node Sizes	95	11, 78	55, 56, 65
Activation	logistic	logistic	logistic
Solver	adam	adam	adam
Alpha	1.00E-03	1.00E-03	1.00E-03
Batch Size	auto	auto	auto
Learning Rate	constant	constant	constant
Learning Rate Init	1.00E-03	1.00E-03	1.00E-03
Max iterations	2000	2000	2000
Tolerance	1.00E-04	1.00E-04	1.00E-04
Tuning Time (minute)	22	38	44
Train: RMSE, SD (N)	0.338, 0.028	0.338, 0.031	0.329, 0.015
Test: RMSE, SD (N)	0.366, 0.031	0.368, 0.037	0.365, 0.031

3.3.3 Fourth preliminary: prediction accuracy performance of optimized models under various window sizes

According to Baig *et al.,* [43], accurately predicting force based on sEMG is challenging due to the dynamic nature of the human environment. Using a fixed window size for data stream mining may not yield precise results, as it depends on specific models and system characteristics. Choosing an appropriate window size is crucial to avoid inaccurate estimations and maintain predictive

performance. A set of experiments were conducted to determine the appropriate window size for Ridge Polynomial, ANN, and SVM models in sEMG-based force estimation. The tests involved the same group of participants performing HMI tasks with varying sample sizes of 10, 50, 100, 150, 200, and 250.

Hyperparameter tuning was performed for all cases, and the qualitative performance of the model predictions was evaluated based on the RMSE values. A lower RMSE value indicates improved prediction accuracy. Table 4 presents the prediction accuracy performance of the optimized models (Ridge Polynomial, SVM, and ANN) under various window sizes. The results indicate that the choice of window size does not significantly impact the prediction capabilities, as the RMSE values are relatively similar. The RMSE values for the Ridge Polynomial, SVM, and ANN models range from 0.38 to 0.40 N, 0.35 to 0.37 N, and 0.34 to 0.36 N, respectively.

All optimized models, with their respective hyperparameter tuning, demonstrate acceptable accuracy for sEMG-based force estimation and provide effective compensation for gravity and intrinsic muscular force. Upon careful observation, it can be concluded that the ANN model exhibits better overall performance and slightly outperforms the SVM and Ridge Polynomial techniques. Additionally, the SVM model exhibited certain disadvantages in terms of longer training and testing durations, ranging from 32 to 168 seconds for training and 24 to 28 seconds for testing. The window size of 10 resulted in the longest duration.

Table 4
The comparison results of machine learning optimize models under different window sizes of datasets

ML	Window size											
Algorithm	10		50		100		150		200		250	
Ridge-Polynomial	Train	Test	Train	Test	Train	Test	Train	Test	Train	Test	Train	Test
RMSE (N)	0.356	0.377	0.341	0.380	0.337	0.387	0.334	0.397	0.331	0.400	0.329	0.400
SD (N)	0.009	0.029	0.011	0.034	0.013	0.030	0.011	0.012	0.009	0.014	0.009	0.018
*Time (second)	0.045	0.025	0.046	0.027	0.048	0.031	0.045	0.026	0.044	0.025	0.052	0.027
Support Vector Machine	Train	Test	Train	Test	Train	Test	Train	Test	Train	Test	Train	Test
RMSE (N)	0.319	0.347	0.314	0.356	0.300	0.373	0.297	0.361	0.304	0.367	0.308	0.371
SD (N)	0.014	0.040	0.014	0.035	0.013	0.019	0.013	0.020	0.011	0.013	0.010	0.018
*Time (second)	168.1	26.38	35.73	28.64	44.16	28.05	32.81	26.54	33.36	25.72	31.66	24.38
Neural Network	Train	Test	Train	Test	Train	Test	Train	Test	Train	Test	Train	Test
RMSE (N)	0.325	0.344	0.323	0.353	0.318	0.356	0.318	0.348	0.321	0.348	0.317	0.354
SD (N)	0.014	0.047	0.015	0.041	0.013	0.029	0.011	0.030	0.012	0.032	0.013	0.031
*Time (second)	1.280	0.052	2.699	0.045	1.204	0.017	0.751	0.007	0.948	0.005	0.698	0.007

*Note: The train time is second per 40,000 samples and the predict time is second per 10,000 samples.

On the other hand, the training and testing durations for the Ridge Polynomial model fluctuated slightly, ranging from 0.044 to 0.052 seconds and 0.025 to 0.031 seconds, respectively. In contrast, the window sizes had a significant impact on the training and testing durations in the ANN model. Smaller window sizes corresponded to quicker processing times. The best performance, as determined by the ANN model, was achieved with a window size of 200. It yielded an RMSE of 0.321 N (with a corresponding standard deviation of 0.012) for training and 0.345 N (with an SD of 0.032) for testing.

In summary, the optimized ANN model, which exhibited superior performance in sEMG-based force estimation, was employed in a substantive experiment. The model's accuracy, with low RMSE values for training and testing, makes it a reliable choice for the experiment's objectives.

4. Substantive results and discussion

4.1 Substantive Experiment: Comparison of Novel Technique with Conventional Method for Robot-Assisted Upper-Limb Rehabilitation

To simulate a real-world upper-limb rehabilitation scenario, a substantive set of robot-assisted rehabilitation tests was conducted with the same group of participants. The ANN model was employed to facilitate the CPM robot with the compensation of gravity and time-varying intrinsic muscular force. The parameters for optimizing the ANN were configured as follows: a single hidden layer with 11 nodes, the logistic activation function, and the Adam optimizer as the solver. The objective was to measure the net force exerted on the test rig while the participant maintained a state of rest without applying any voluntary effort throughout the CPM process ($F_{RES} = 0$).

In these tests, participants were familiarized with the test rig to minimize the influence of human learning factors. Each subject had to place the forearm and elbow at the arm supporter. It can be claimed that in the absence of voluntary force exerted on the test rig, the system should accurately measure the total external force, aiming for a value as close to zero as possible. Hence, the performance of the system's natural response was evaluated by analysing the variation in calculated voluntary forces acting on the test rig. A lower variation in calculated voluntary forces indicated a better performance of the system.

Figure 5 presents a comparison of the results obtained by employing only conventional gravity compensation and our novel technique, which integrates both intrinsic muscular force and gravity compensation. The performance of the system is indicated by the close approximation of calculated forces to zero throughout the process, aligning with the expected physical behaviour of patients who exert no voluntary power. The findings demonstrate that our technique yields a lower variation in calculated voluntary forces compared to the conventional method. Notably, our technique achieves an average RMSE of 0.43 N, surpassing the performance of the conventional method with an average RMSE of 1.48 N.

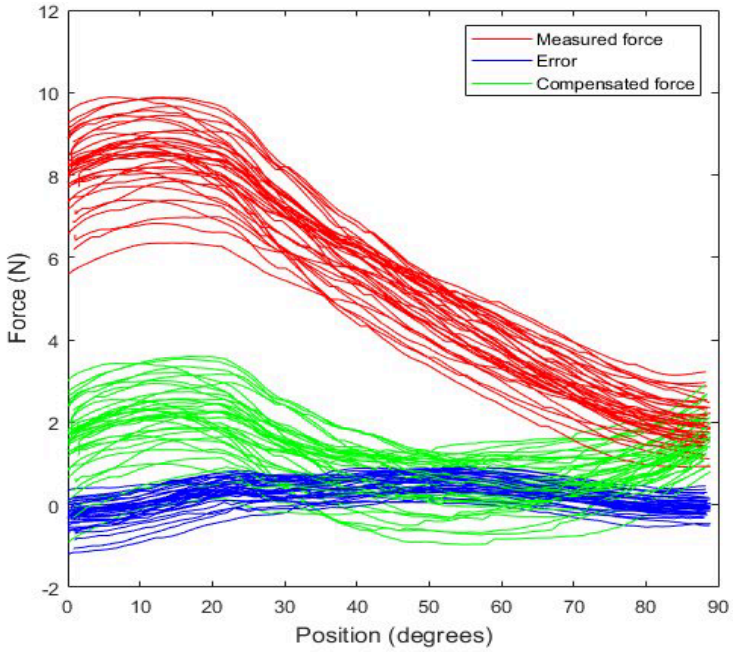

Fig. 5. The compared results between the conventional gravity compensation and our novel technique using gravity and intrinsic muscular force compensation when patients exert no voluntary power

A practical real experiment was further conducted to validate the effectiveness of the robotic-human-like controller with high-accuracy measurement of voluntary forces for CPM. The same group of participants were instructed to simulate the experience of intense pain during CPM therapy by applying voluntary resistant force against the robotic movement. Figure 6 depicts the behaviour of the CPM robotic movement throughout the treatment process. It can be clearly seen that in the absence of voluntary resistance, the single rotational DOF results in a consistent circular-path movement at a constant speed of 3 rpm. Once the participants simulate the experience of pain, they generate voluntary resistant force. In real-time response, the CPM robot promptly adjusts the motion speed, aiming to mimic natural behavioural responses. The graph demonstrates a decrease in speed towards zero while the resistant force steadily increases during severe pain.

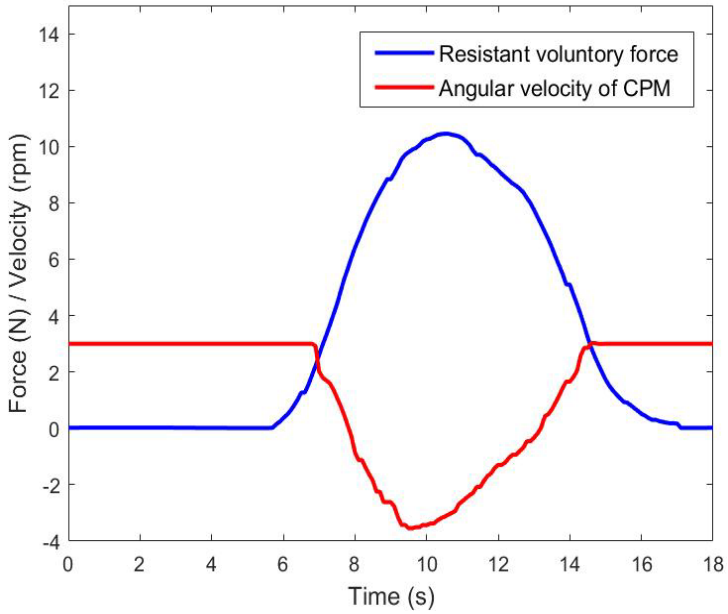

Fig. 6. The natural behavioral response of the developed CPM robot with prompt adjustments of lower speed of motion in response to the voluntary resistant exertion

In cases where the applied voluntary force exceeds a certain threshold, this adjustment prevents the occurrence of potential physical injuries by causing the CPM bar to move backwards, away from the participant. Once the situation returns to normal and the applied voluntary force approaches zero, the CPM system returns to its regular state and resumes manipulating the human forearm. It still maintains a constant angular velocity of 3 rpm to complete a CPM therapy cycle.

In summary, the ANN model successfully compensated for gravity and intrinsic muscular force in a robot-assisted rehabilitation scenario. It achieved accurate measurements of net force and demonstrated superior performance compared to conventional methods. The system effectively adjusted motion speed in response to voluntary resistance, providing high-accuracy measurement and appropriate adjustments during therapy. Nevertheless, when implemented in real-world scenarios, the device exhibits some limitations. Specifically, its response to voluntary resistance may require additional fine-tuning to adapt to the spectrum of patient effort levels. Moreover, when operational with real patients, the machine learning component should iteratively learn to remodel accurately based on real-time interactions.

5. Conclusion

In conclusion, this research contributes to the development of a robotic-human-like controller with high-accuracy measurement of voluntary forces for CPM. This addresses a significant research gap related to natural behavioural responses in robotic CPM rehabilitation. The developed system effectively compensates for irrelevant forces, such as gravity and intrinsic muscular force, acting on the test rig. Careful preprocessing and model optimization techniques were applied, showcasing that the ANN method slightly outperforms others, enhancing accuracy and precision while boasting quicker testing times. The substantial findings also underscore a noteworthy comparison between traditional gravity compensation and our innovative approach, which integrates both intrinsic muscular force and gravity compensation. Notably, our method yields calculated voluntary forces that closely align with actual values, surpassing the accuracy of conventional methods. This allows the CPM robot to accurately track and respond to the voluntary resistant effort in real-time, even in the presence of intense pain during the therapy process. The developed control system ensures compliance with the patient's voluntary resistant force, enhancing the overall effectiveness and safety of the CPM rehabilitation process.

Acknowledgement
This research was supported by Natural Science, Research and Innovation Fund (NSRF) and Prince of Songkla University (Grant No ENG6601188S).

References

[1] Hung, Yu-Hsiu, Pin-Ju Chen, and Wan-Zi Lin. "Design factors and opportunities of rehabilitation robots in upper-limb training after stroke." In *2017 14th International Conference on Ubiquitous Robots and Ambient Intelligence (URAI)*, pp. 650-654. IEEE, 2017. https://doi.org/10.1109/URAI.2017.7992694

[2] Gopura, Ruwan ARC, and Kazuo Kiguchi. "Mechanical designs of active upper-limb exoskeleton robots: State-of-the-art and design difficulties." In *2009 IEEE International Conference on Rehabilitation Robotics*, pp. 178-187. IEEE, 2009. https://doi.org/10.1109/ICORR.2009.5209630

[3] Zhang, Xue, Zan Yue, and Jing Wang. "Robotics in lower-limb rehabilitation after stroke." *Behavioural neurology* 2017, no. 1 (2017): 3731802. https://doi.org/10.1155/2017/3731802

[4] Koeppel, T., and O. Pila. "Test-retest reliability of kinematic assessments for upper limb robotic rehabilitation." *IEEE Transactions on Neural Systems and Rehabilitation Engineering* 28, no. 9 (2020): 2035-2042. https://doi.org/10.1109/TNSRE.2020.3013705

[5] Song, Rong, Kai-yu Tong, Xiaoling Hu, and Le Li. "Assistive control system using continuous myoelectric signal in robot-aided arm training for patients after stroke." *IEEE transactions on neural systems and rehabilitation engineering* 16, no. 4 (2008): 371-379. https://doi.org/10.1109/TNSRE.2008.926707

[6] Maciejasz, Paweł, Jörg Eschweiler, Kurt Gerlach-Hahn, Arne Jansen-Troy, and Steffen Leonhardt. "A survey on robotic devices for upper limb rehabilitation." *Journal of neuroengineering and rehabilitation* 11 (2014): 1-29. https://doi.org/10.1186/1743-0003-11-3

[7] McDonald, Craig G., Jennifer L. Sullivan, Troy A. Dennis, and Marcia K. O'Malley. "A myoelectric control interface for upper-limb robotic rehabilitation following spinal cord injury." *IEEE Transactions on Neural Systems and Rehabilitation Engineering* 28, no. 4 (2020): 978-987. https://doi.org/10.1109/TNSRE.2020.2979743

[8] Nakayama, Takayuki, Yousuke Araki, and Hideo Fujimoto. "A new gravity compensation mechanism for lower limb rehabilitation." In *2009 international conference on mechatronics and automation*, pp. 943-948. IEEE, 2009. https://doi.org/10.1109/ICMA.2009.5246352

[9] Smith, Richard L., Joan Lobo-Prat, Herman van der Kooij, and Arno HA Stienen. "Design of a perfect balance system for active upper-extremity exoskeletons." In 2013 IEEE 13th International Conference on Rehabilitation Robotics (ICORR), pp. 1-6. IEEE, 2013. https://doi.org/10.1109/ICORR.2013.6650376

[10] Bamdad, Mahdi, and Farhad Parivash. "Integrated active and passive gravity compensation method for a cable-actuated elbow rehabilitation robot." In *2015 3rd RSI international conference on robotics and mechatronics (ICROM)*, pp. 079-084. IEEE, 2015. https://doi.org/10.1109/ICRoM.2015.7367764

[11] Spagnuolo, Giulio, Matteo Malosio, Alessandro Scano, Marco Caimmi, Giovanni Legnani, and Lorenzo Molinari Tosatti. "Passive and active gravity-compensation of LIGHTarm, an exoskeleton for the upper-limb rehabilitation." In *2015 IEEE international conference on rehabilitation robotics (ICORR)*, pp. 440-445. IEEE, 2015. https://doi.org/10.1109/ICORR.2015.7281239

[12] Just, Fabian, Özhan Özen, Stefano Tortora, Verena Klamroth-Marganska, Robert Riener, and Georg Rauter. "Human arm weight compensation in rehabilitation robotics: efficacy of three distinct methods." *Journal of neuroengineering and rehabilitation* 17 (2020): 1-17. https://doi.org/10.1186/s12984-020-0644-3

[13] Peng, Liang, Zeng-Guang Hou, and Weiqun Wang. "Dynamic modeling and control of a parallel upper-limb rehabilitation robot." In *2015 IEEE International Conference on Rehabilitation Robotics (ICORR)*, pp. 532-537. IEEE, 2015. https://doi.org/10.1109/ICORR.2015.7281254

[14] O'Driscoll, S. W., A. Kumar, and R. B. Salter. "The effect of the volume of effusion, joint position and continuous passive motion on intraarticular pressure in the rabbit knee." *The Journal of Rheumatology* 10, no. 3 (1983): 360-363.

[15] Lobo-Prat, Joan, Peter N. Kooren, Mariska MHP Janssen, Arvid QL Keemink, Peter H. Veltink, Arno HA Stienen, and Bart FJM Koopman. "Implementation of EMG-and force-based control interfaces in active elbow supports for men with duchenne muscular dystrophy: A feasibility study." *IEEE transactions on neural systems and rehabilitation engineering* 24, no. 11 (2016): 1179-1190. https://doi.org/10.1109/TNSRE.2016.2530762

[16] Neranon, Paramin, and Robert Bicker. "Force/position control of a robot manipulator for human-robot interaction." *Thermal Science* 20, no. suppl. 2 (2016): 537-548. https://doi.org/10.2298/TSCI151005036N

[17] Neranon, Paramin, and Tanapong Sutiphotinun. "A human-inspired control strategy for improving seamless robot-to-human handovers." *Applied Sciences* 11, no. 10 (2021): 4437. https://doi.org/10.3390/app11104437

[18] Neranon, Paramin. "Implicit force control approach for safe physical robot-to-human object handover." *Indonesian J. Electric. Eng. Comput. Sci* 17 (2020): 615-628. https://doi.org/10.11591/ijeecs.v17.i2.pp615-628

[19] Jaroonsorn, Prakarn, Paramin Neranon, Pruittikorn Smithmaitrie, and Charoenyutr Dechwayukul. "Robot-assisted transcranial magnetic stimulation using hybrid position/force control." *Advanced Robotics* 34, no. 24 (2020): 1559-1570. https://doi.org/10.1080/01691864.2020.1855243

[20] Gao, Fan, Yupeng Ren, Elliot J. Roth, Richard Harvey, and Li-Qun Zhang. "Effects of repeated ankle stretching on calf muscle–tendon and ankle biomechanical properties in stroke survivors." *Clinical biomechanics* 26, no. 5 (2011): 516-522. https://doi.org/10.1016/j.clinbiomech.2010.12.003

[21] Kaewboon, Wansitta, Pornchai Phukpattaranont, and Chusuk Limsakul. "Upper limbs rehabilitation system for stroke patient with biofeedback and force." In *The 6th 2013 Biomedical Engineering International Conference*, pp. 1-5. IEEE, 2013. https://doi.org/10.1109/BMEiCon.2013.6687651

[22] World Medical Association. "World Medical Association Declaration of Helsinki: ethical principles for medical research involving human subjects." *Jama* 310, no. 20 (2013): 2191-2194. https://doi.org/10.1001/jama.2013.281053

[23] Ekinci, Serdar, Baran Hekimoğlu, and Davut Izci. "Opposition based Henry gas solubility optimization as a novel algorithm for PID control of DC motor." *Engineering Science and Technology, an International Journal* 24, no. 2 (2021): 331-342. https://doi.org/10.1016/j.jestch.2020.08.011

[24] Tanausavaphol, Tanat, Paramin Neranon, Passakorn Vessakosol, and Pornchai Phukpattaranont. "EMG–Based force estimation for dynamic muscle contractions in physical human-robot interaction." *J Mech Eng Res Dev* 43, no. 2 (2020): 165-177.

[25] Kim, Hyo Jin, Ye Sol Lee, and Donghan Kim. "Arm motion estimation algorithm using MYO armband." In *2017 First IEEE International Conference on Robotic Computing (IRC)*, pp. 376-381. IEEE, 2017. https://doi.org/10.1109/IRC.2017.32

[26] Liang, Peidong, Chenguang Yang, Ning Wang, and Ruifeng Li. "A Discrete-Time Algorithm for Stiffness Extraction from sEMG and Its Application in Antidisturbance Teleoperation." *Discrete Dynamics in Nature and Society* 2016, no. 1 (2016): 6897030. https://doi.org/10.1155/2016/6897030

[27] Rahman, M. M., R. Ikeura, and K. Mizutani. "Investigating the impedance characteristic of human arm for development of robots to co-operate with human operators." In *IEEE SMC'99 Conference Proceedings. 1999 IEEE International Conference on Systems, Man, and Cybernetics (Cat. No. 99CH37028)*, vol. 2, pp. 676-681. IEEE, 1999. https://doi.org/10.1109/ICSMC.1999.825342

[28] Rahman, Md Mozasser, Ryojun Ikeura, and Kazuki Mizutani. "Investigation of the impedance characteristic of human arm for development of robots to cooperate with humans." *JSME International Journal Series C Mechanical Systems, Machine Elements and Manufacturing* 45, no. 2 (2002): 510-518. https://doi.org/10.1299/jsmec.45.510

[29] PJaroonsorn, Prakarn, Paramin Neranon, Charoenyut Dechwayukul, and Pruittikorn Smithmaitrie. "Performance comparison of compliance control based on pi and FLC for safe human-robot cooperative object carrying." In *2019*

First International Symposium on Instrumentation, Control, Artificial Intelligence, and Robotics (ICA-SYMP), pp. 13-16. IEEE, 2019. https://doi.org/10.1109/ICA-SYMP.2019.8646008

[30] Kececi, Aybuke, Armağan Yildirak, Kaan Ozyazici, Gulsen Ayluctarhan, Onur Agbulut, and Ibrahim Zincir. "Implementation of machine learning algorithms for gait recognition." *Engineering Science and Technology, an International Journal* 23, no. 4 (2020): 931-937. https://doi.org/10.1016/j.jestch.2020.01.005

[31] Okafor, Christian Emeka, Ezekiel Junior Okafor, and Kingsley Okechukwu Ikebudu. "Evaluation of machine learning methods in predicting optimum tensile strength of microwave post-cured composite tailored for weight-sensitive applications." *Engineering Science and Technology, an International Journal* 25 (2022): 100985. https://doi.org/10.1016/j.jestch.2021.04.004

[32] Simao, Miguel, Nuno Mendes, Olivier Gibaru, and Pedro Neto. "A review on electromyography decoding and pattern recognition for human-machine interaction." *Ieee Access* 7 (2019): 39564-39582. https://doi.org/10.1109/ACCESS.2019.2906584

[33] Behera, N. K. S., and H. S. Behera. "Firefly based ridge polynomial neural network for classification." In *2014 IEEE international conference on advanced communications, control and computing technologies*, pp. 1110-1113. IEEE, 2014. https://doi.org/10.1109/ICACCCT.2014.7019270

[34] Voutriaridis, Christodoulos, Yiannis S. Boutalis, and Basil G. Mertzios. "Ridge polynomial networks in pattern recognition." In *Proceedings EC-VIP-MC 2003. 4th EURASIP Conference focused on Video/Image Processing and Multimedia Communications (IEEE Cat. No. 03EX667)*, vol. 2, pp. 519-524. IEEE, 2003. https://doi.org/10.1109/VIPMC.2003.1220516

[35] Khoshdel, Vahab, and Alireza Akbarzadeh. "An optimized artificial neural network for human-force estimation: consequences for rehabilitation robotics." *Industrial Robot: An International Journal* 45, no. 3 (2018): 416-423. https://doi.org/10.1108/IR-10-2017-0190

[36] Hu, Jin, Zengguang Hou, Feng Zhang, Yixiong Chen, and Pengfeng Li. "Training strategies for a lower limb rehabilitation robot based on impedance control." In *2012 Annual International Conference of the IEEE Engineering in Medicine and Biology Society*, pp. 6032-6035. IEEE, 2012. https://doi.org/10.1109/EMBC.2012.6347369

[37] Reddy, M. Jaya Bharata, P. Gopakumar, and D. K. Mohanta. "A novel transmission line protection using DOST and SVM." *Engineering Science and Technology, an International Journal* 19, no. 2 (2016): 1027-1039. https://doi.org/10.1016/j.jestch.2015.12.011

[38] Smidstrup, A., E. Erkocevic, M. J. Neimeier, M. F. Bøg, J. C. Rosenvang, and Ernest Nlandu Kamavuako. "A comparison study of EMG features for force prediction." In *MEC 11 Raising the Standard—Proc. of the 2011 MyoElectric Controls/Powered Prosthetics Symp*, pp. 93-6. 2011.

[39] J. Snoek, H. Larochelle, and R. P. Adams, "Practical Bayesian Optimization of Machine Learning Algorithms," in *Advances in Neural Information Processing Systems*, Curran Associates, Inc., 2012. Accessed: Jul. 13, 2023. [Online].

[40] Mahmood, Noof T., Mahmuod Hamza Al-Muifraje, Thamir R. Saeed, and Assel H. Kaittan. "Upper prosthetic design based on EMG: A systematic review." In *IOP Conference Series: Materials Science and Engineering*, vol. 978, no. 1, p. 012025. IOP Publishing, 2020. https://doi.org/10.1088/1757-899X/978/1/012025

[41] Karlik, Bekir. "Machine learning algorithms for characterization of EMG signals." *International Journal of Information and Electronics Engineering* 4, no. 3 (2014): 189. https://doi.org/10.7763/IJIEE.2014.V4.433

[42] Shahriari, Bobak, Kevin Swersky, Ziyu Wang, Ryan P. Adams, and Nando De Freitas. "Taking the human out of the loop: A review of Bayesian optimization." *Proceedings of the IEEE* 104, no. 1 (2015): 148-175. https://doi.org/10.1109/JPROC.2015.2494218

[43] Iqbal, Waheed, Josep Lluis Berral, and David Carrera. "Adaptive sliding windows for improved estimation of data center resource utilization." *Future Generation Computer Systems* 104 (2020): 212-224. https://doi.org/10.1016/j.future.2019.10.026